

A&A manuscript no.
(will be inserted by hand later)

Your thesaurus codes are:
(12.04.2; 13.25.3)

ASTRONOMY
AND
ASTROPHYSICS

The BeppoSAX 1-8 keV cosmic background spectrum

A. Vecchi¹, S. Molendi¹, M. Guainazzi², F. Fiore³, and A.N. Parmar²

¹ Istituto di Fisica Cosmica “G.Occhialini”, Via Bassini 15, I-20133 Milano, Italy

² Astrophysics Division, Space Science Department of ESA, ESTEC, Postbus 299, 2200 AG Noordwijk, The Netherlands

³ BeppoSAX Science Data Center, Nuova Telespazio, via Corcolle 19 I-00131 Roma, Italy

the date of receipt and acceptance should be inserted later

Abstract. The spectrum of the 1.0–8.0 keV cosmic X-ray background (CXB) at galactic latitudes $>|25|^\circ$ has been measured using the BeppoSAX LECS and MECS instruments. The spectrum is consistent with a power-law of photon index 1.40 ± 0.04 and normalization 11.7 ± 0.5 photon $\text{cm}^{-2} \text{s}^{-1} \text{keV}^{-1} \text{sr}^{-1}$ at 1 keV. Our results are in good agreement with previous ROSAT PSPC (Georgantopoulos et al. 1996), ASCA GIS (Miyaji et al. 1998) and rocket (McCammon & Sanders 1990) measurements. On the contrary, previous measurements with the HEAO1 A2 (Marshall et al. 1980) and the ASCA SIS (Gendreau et al. 1995) instruments, are characterized by normalizations which are respectively 35% and 25% smaller than ours.

Key words: diffuse radiation – X-rays: General

1. Introduction

The first measurement of the cosmic X-ray background (CXB) dates back to the early 60s (Giacconi et al. 1962). This serendipitous discovery posed the still unsolved problem of the origin of the CXB. Later observations (e.g. Schwartz & Gursky 1974) have shown that the CXB above 1 keV is highly isotropic. This, as well as other evidence, has led to the current understanding that the CXB, at energies above 1 keV, is of extragalactic origin. High angular resolution X-ray observations, and the absence of distortions in the cosmic microwave background spectrum (Fixsen et al. 1996), support the idea that the CXB above 1 keV is dominated by the integrated emission from faint sources, with a dominant contribution coming from Active Galactic Nuclei (AGN). Recent results from X-ray surveys show that the fraction of the CXB due to discrete sources is 70–80% in the 0.5–2.0 keV band (Hasinger et al. 1998) and at least 30% in the 2–10 keV band (Fiore et al. 1999). The CXB spectrum in the 3–50 keV band, measured by HEAO1 A2 (Marshall et al. 1980), is adequately represented by a power-law with an exponential cutoff at ~ 40 keV. In

the 2–10 keV energy range the CXB spectrum is approximated by a power-law with photon index 1.4. Further measurements of the CXB spectrum, performed with the ROSAT PSPC (Hasinger 1992) in the 0.5–2.0 keV band, with the ASCA SIS (Gendreau et al. 1995) in the 0.4–7.0 keV band, and with the ASCA GIS (Miyaji et al. 1998) in the 1.0–10.0 keV band, disagree at about the 20%–30% level as to the value of the 1 keV normalization. While the ASCA GIS and ROSAT PSPC measurements give values around $11 \text{ photon s}^{-1} \text{cm}^{-2} \text{keV}^{-1} \text{sr}^{-1}$, the ASCA SIS spectrum, which lies on the extrapolation of the HEAO1 A2 measurement, yields a value of $\sim 9 \text{ photon s}^{-1} \text{cm}^{-2} \text{keV}^{-1} \text{sr}^{-1}$. New observations of the CXB spectrum are needed to clarify the issue.

In this letter we present a new measurement of the CXB spectrum, in the 1.0–8.0 keV, obtained with the LECS and MECS instruments on board BeppoSAX. A previous measurement, using LECS data alone, has been presented by Parmar et al. (1999; P99 hereinafter). The remainder of the letter is organized as follows. In Sect. 2 we discuss instrumental issues relevant to the analysis of the LECS and MECS CXB spectra. In Sect. 3 we present the list of observations which have been used to measure the CXB spectrum. In Sect. 4 we report on the spectral analysis. In Sect. 5 we discuss our findings and compare them to previous results.

2. Instrumental issues

2.1. LECS

The Low-Energy Concentrator Spectrometer (LECS; 0.1–10 keV; Parmar et al. 1997) is an imaging scintillation proportional counter on-board the Italian-Dutch BeppoSAX X-ray astronomy mission (Boella et al. 1997a). It has a circular field of view of $18.5'$ radius, an effective area of $\simeq 40 \text{ cm}^2$ at 2 keV and an energy resolution of $\simeq 8\%$ at 6 keV. Details on the CXB data reduction can be found in P99. Briefly, the CXB was accumulated within a central circle with an $8'$ radius. The spectrum of the non X-ray background (NXB) has been accumulated during 816.3 ks of dark Earth pointing (this is a factor 1.6 greater than in P99). The response matrix we employ is the same used

by P99. Briefly, we recall that the response matrix, which is appropriate for the diffuse emission, has been generated, by simulating a set of 100 point sources, randomly distributed within a radius of $12'$, therefore larger than the CXB accumulation region. This matrix includes also the effect of off-axis mirror vignetting and the average obscuration of the support strongback. Moreover the LECS matrix has been corrected for the $\sim 15\%$ LECS/MECS crosscalibration mismatch present in the September 1997 release of BeppoSAX matrices. We expect any residual crosscalibration error between LECS and MECS to be less than $\sim 5\%$. In addition to the above effects, single reflected X-rays from within $120'$ can be detected in the FOV (Conti et al. 1994). The magnitude of this effect has been found to be $< 1\%$ of the flux within an $8'$ extraction radius (P99). Since this is well within the uncertainty in CXB normalization, this effect is ignored.

2.2. MECS

The Medium-Energy Concentrator Spectrometer (MECS; 1.5–10 keV; Boella et al. 1997b) is an imaging gas scintillation proportional counter. The MECS was originally composed of 3 units, MECS1, MECS2 and MECS3. MECS1 failed in May 1997, in this paper we shall use only data from the 2 units which are still operative. The energy resolution is 8% at 6 keV. The combined on-axis effective area for the MECS2 and MECS3 units is $\sim 80 \text{ cm}^2$ at 2.0 keV and $\sim 60 \text{ cm}^2$ at 8 keV. The MECS has a circular field of view (FOV) of $25'$ radius. An annular support structure, commonly referred to as strongback, is localized at about $10'$ from the center of the detector. The absolute flux calibration of the MECS was performed using the Crab nebula spectrum. Assuming a power-law model the photon index, α , and the 2-10 keV flux, $F(2-10)$, for the Crab, are found to be $\alpha = 2.088 \pm 0.002$ and $F(2-10) = 2.008 \pm 0.006 \times 10^{-8} \text{ erg cm}^{-2} \text{ s}^{-1}$. Repeated observations have not revealed any significant variations in either of these parameters so far (Sacco 1999). The uncertainty in the line of sight N_{H} for the Crab, may affect at the few percent level the MECS calibration in the softest (1.65–2.0 keV) energy band. For the present work we have chosen to accumulate spectra from a relatively small central circular region with radius $8'$. The main reasons for this choice are that: *i*) the ratio of the CXB to the NXB is at its highest at the center of the detector; *ii*) we avoid complications associated to the obscuration from the strongback; *iii*) the inner region of the MECS detector is better calibrated than the outer one. We have created a response matrix appropriate for uniform diffuse emission. This matrix differs from the standard point-source response matrix in the following ways: *i*) the effects of off-axis mirror vignetting are included; *ii*) the CXB is modeled as a uniform diffuse emission, within a radius of $12'$. The MECS response matrix has been generated using the EFFAREA program publically available within the latest SAXDAS

release. The NXB accounts for a significant fraction of the total background, thus a correct measurement of the NXB is needed to measure the CXB. A total of 1850 ks of NXB data was accumulated using MECS dark Earth pointings. In the central $8'$ the MECS NXB spectrum is approximately constant with energy, with a count rate of $4 \times 10^{-4} \text{ cts s}^{-1} \text{ keV}^{-1} \text{ MECS}^{-1}$, between 1.0 and 4.5 keV. Between 4.5 keV and 7 keV there is a smooth increase in count rate with 3 discrete line-like features superposed. Above 7 keV the spectrum is again flat with a count rate of $8 \times 10^{-4} \text{ cts s}^{-1} \text{ keV}^{-1} \text{ MECS}^{-1}$. Above $\sim 8 \text{ keV}$, the NXB dominates the overall background spectrum. Due to the low-inclination, almost circular, BeppoSAX orbit, variations in the NXB counting rate around the orbit are negligible.

3. CXB observations

A background spectrum, with a total exposure time of 694.2 ks for the LECS (a factor 1.25 greater than in P99) and 1574.8 ks for the MECS, was accumulated from a number of high galactic latitude exposures by extracting counts within an $8'$ radius of the nominal source position within the LECS and MECS FOV (Table 1). While a light leakage problem has forced us to use the LECS only during night time, the MECS data has been accumulated during day and night time. For various reasons of the 16 pointing listed 4 have only MECS data and 3 have only LECS data. We note that the total integration times, the covered solid angles (0.67 sq deg for the LECS, and 0.73 sq deg for the MECS) and most importantly the accumulated photons (more than 44000 for the LECS plus MECS), are larger than those associated to previous measurements of the CXB spectrum, with imaging instruments, in the medium energy band. For this reason we expect our measurement to be limited by systematic effects rather than by counting statistics or by fluctuations associated to the CXB granularity. No point sources are present in the individual fields with 0.1–2.0 keV fluxes $> 1.7 \times 10^{-13} \text{ erg cm}^{-2} \text{ s}^{-1}$, and with 2.0–10.0 keV fluxes $> 5 \times 10^{-13} \text{ erg cm}^{-2} \text{ s}^{-1}$. Using the 2-10 keV LogN-LogS reported in Comastri et al. (1999) we have estimated that about 5% of the total CXB is produced by source above the $5 \times 10^{-13} \text{ erg cm}^{-2} \text{ s}^{-1}$ flux limit. All the fields have galactic latitudes $> |25^\circ|$ and galactic column densities between 2.0 and $7.0 \times 10^{20} \text{ atom cm}^{-2}$. The spectrum was rebinned to have at least 20 counts per bin in order to ensure the applicability of the χ^2 statistic. All uncertainties are quoted at the 90% confidence level for one interesting parameter ($\Delta\chi^2 = 2.7$).

4. X-ray background spectrum

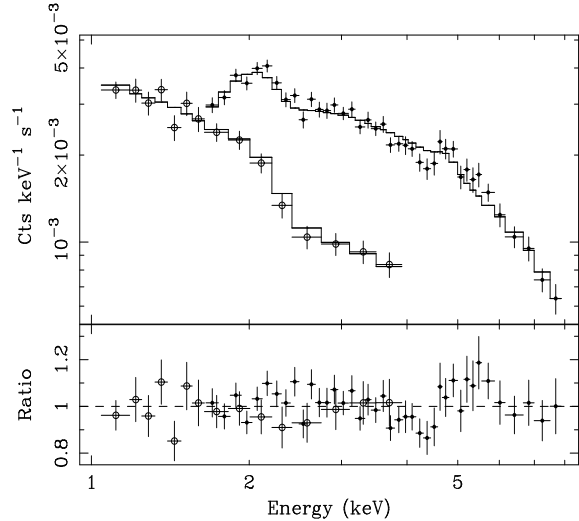
Spectral fitting has been performed using the 1.0–4.0 keV LECS spectrum and the 1.65–8.0 keV MECS spectrum (as customary we have equalized MECS2 and MECS3 data

Table 1. BeppoSAX observations used to create the CXB spectrum. N_{gal} is the line of sight absorption in units of $10^{20} \text{ atom cm}^{-2}$ (Dickey & Lockman 1990)

Pointing (J2000)		l_{II} ($^{\circ}$)	b_{II} ($^{\circ}$)	Observations		$T_{\text{exp}}^{\text{LECS}}$ (ks)	$T_{\text{exp}}^{\text{MECS}}$ (ks)	N_{gal}
RA (h m s)	Dec ($^{\circ}$ ' ")			Start (yr mn day)	Stop (yr mn day)			
01 39 35.4	+89 14 06	123.1	+26.4	1997 Feb 01	1997 Feb 03	...	115.5	6.8
02 31 42.0	+89 15 47	123.4	+26.5	1996 Jul 01	1997 May 23	69.7	257.8	7.0
05 52 07.9	-61 05 35	270.0	-30.6	1998 Mar 10	1998 Mar 22	46.7	156.6	5.3
06 12 22.7	-60 59 04	270.1	-28.2	1996 Oct 10	1996 Oct 12	43.3	115.0	4.2
06 22 36.4	-69 15 28	279.5	-27.8	1998 Oct 23	1998 Oct 23	12.4	34.4	6.9
16 35 10.7	+59 46 30	89.9	+40.2	1996 Aug 27	1996 Aug 31	79.9	170.4	2.0
16 51 19.5	+60 11 49	89.8	+38.1	1996 Aug 23	1996 Aug 27	82.3	...	2.1
17 30 42.2	+60 55 32	89.9	+33.2	1996 Aug 21	1996 Aug 23	...	65.8	3.5
17 38 57.1	+68 01 10	98.2	+31.8	1999 Mar 03	1999 Mar 03	20.5	...	4.4
17 49 33.7	+61 05 54	90.0	+30.9	1998 Mar 28	1998 Mar 29	...	53.4	3.5
17 50 51.1	+61 05 45	90.0	+30.8	1998 Sep 10	1999 Apr 11	88.1	49.8	3.5
17 52 07.4	+61 01 01	89.9	+30.6	1998 Aug 22	1998 Oct 07	116.6	206.0	3.5
17 56 46.1	+61 11 45	90.2	+30.1	1997 Mar 23	1997 Mar 25	94.2	116.7	3.4
17 58 14.6	+61 12 30	90.2	+29.9	1997 Mar 18	1997 Mar 20	...	119.0	3.4
18 18 20.5	+60 58 42	90.2	+27.4	1997 Apr 13	1997 Apr 15	26.6	114.4	3.8
23 07 53.5	+08 50 06	84.4	-46.1	1997 Dec 13	1997 Dec 14	13.9	...	4.7

and produced a single MECS spectrum). Data below 1.0 keV is ignored as we are interested in characterizing the extragalactic CXB. LECS data above 4.0 keV, where a slight miscalibration problem is present, has also been ignored. MECS data above 8.0 keV, where the NXB becomes dominant is also ignored. All spectral models have been absorbed by a foreground column density, N_{H} , of $3.8 \times 10^{20} \text{ atom cm}^{-2}$, which has been derived by averaging the galactic densities of the blank fields listed in Table 1. In all fits we have allowed for a maximum cross calibration mismatch of 5% between LECS and MECS data (see Sect. 2.1). A simple power-law fit gives an acceptable χ^2 of 75.1 for 74 degrees of freedom (dof) with $\alpha = 1.40 \pm 0.04$, a normalization of $11.7 \pm 0.5 \text{ photon s}^{-1} \text{ cm}^{-2} \text{ keV}^{-1} \text{ sr}^{-1}$ at 1 keV and a normalization of $1.70 \pm 0.04 \text{ photon s}^{-1} \text{ cm}^{-2} \text{ keV}^{-1} \text{ sr}^{-1}$ at 4 keV. The normalization at 1 keV is quoted for comparison with previous works, while the normalization at 4 keV is quoted because when using a 1.0-8.0 keV spectral band the most precise determination of the normalization is obtained at the center of the band rather than at one of its limits.

Since a fraction of the 1-2 keV CXB may quite possibly not be of extragalactic origin, we have fitted the CXB spectra with a power-law together with a single temperature optically thin plasma (the Mewe-Kaastra-Liedhal plasma emissivity model in XSPEC, Mewe et al. 1985). Since we are not interested in the thermal component in itself, we fixed its parameters to the best fitting values derived by P99 when fitting the LECS spectrum of the CXB. The power-law plus thermal component fit, which is reported in Fig. 1, gives an acceptable χ^2 of 75.0 for 74 degrees of freedom (dof) with $\alpha = 1.35 \pm 0.04$, a normaliza-

**Fig. 1.** Spectra and residuals in units of the data/model ratio (lower panel) for the power-law plus thermal emission model. Open circles are LECS data, and filled circles are MECS data.

tion of $11.0 \pm 0.5 \text{ photon s}^{-1} \text{ cm}^{-2} \text{ keV}^{-1} \text{ sr}^{-1}$ at 1 keV and a normalization of $1.70 \pm 0.04 \text{ photon s}^{-1} \text{ cm}^{-2} \text{ keV}^{-1} \text{ sr}^{-1}$ at 4 keV. Obviously, the addition of a low energy component has resulted in a reduction of the spectral index and of the 1 keV normalization, while the 4 keV normalization is unaffected.

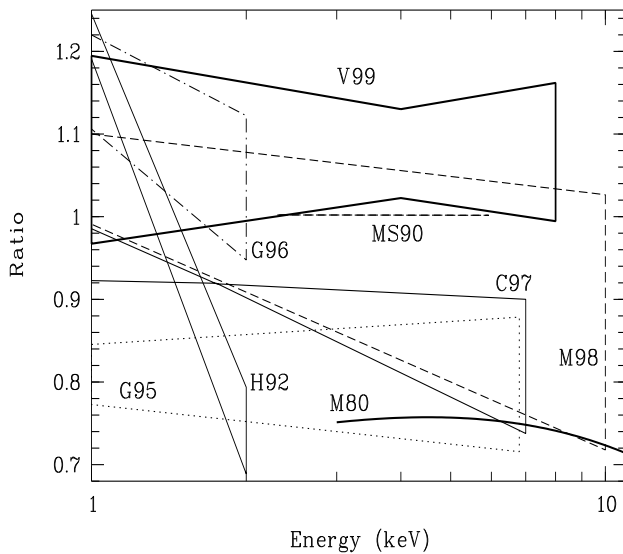


Fig. 2. Ratio of the CXB spectrum to a power-law with photon index 1.4 and normalization at 1 keV of $11 \text{ photon s}^{-1} \text{ cm}^{-2} \text{ keV}^{-1} \text{ sr}^{-1}$. The thick solid line (M80) represents the best fit reported by Gruber et al. (1999) to the HEAO1 A2 measurement by Marshall et al. (1980). The thin solid horn (H92) is the ROSAT PSPC measurement from Hasinger (1992). The dot-dashed horn (G96) is a ROSAT PSPC measurement from Georgantopoulos et al. (1996). The dashed line (MS90) is from rocket measurements (McCammon & Sanders 1990). The dotted horn (G95) is from the ASCA SIS measurement by Gendreau et al. (1995). The long-dashed horn (M98) is the ASCA GIS measurement by Miyaji et al. (1998) on the Lockman Hole. The thin solid bowtie (C97) is a joint ROSAT PSPC ASCA SIS analysis of QSF3 by Chen et al. (1997) for $E > 1 \text{ keV}$. Finally the thick solid bowtie (V99) is our own BeppoSAX LECS and MECS simple power-law fit

5. Discussion

In Fig. 2 we plot various measurements of the CXB spectrum. To facilitate the comparison the spectra are plotted in the form of a ratio of the photon spectrum to a power-law with index 1.4 and normalization at 1 keV of $11 \text{ photon s}^{-1} \text{ cm}^{-2} \text{ keV}^{-1} \text{ sr}^{-1}$. Note that we have associated a 5% error to the normalization of our measurement to account for residual uncertainties in the absolute calibration of the LECS and MECS instruments.

The LECS measurement of P99 is consistent with the LECS-MECS measurement we present here, we have not included the P99 spectrum in Fig.2 to avoid making it even more crowded than it already is. Our measurement is consistent with the ASCA GIS measurement of Miyaji et al. (1998) on the Lockman Hole. Their normalization at 4 keV is smaller than ours by $\sim 13\%$, and within the errors. We are also in agreement with the rocket measure-

ment (McCammon & Sanders 1990) and with the ROSAT PSPC measurement from Georgantopoulos et al. (1996). The joint ROSAT PSPC ASCA SIS analysis of QSF3 by Chen et al. (1997) is in agreement with our measurement at low energies but, due to its steeper spectral index, falls short of our measurement by about 25% at 7 keV. The ASCA SIS measurement of Gendreau et al. (1995) and the HEAO1 measurement of Marshall et al. (1980) have spectral indices similar to ours, but normalizations which are smaller by $\sim 25\%$ and $\sim 30\%$ respectively. The discrepancy with the HEAO1 measurement is somewhat larger, $\sim 35\%$ if we consider the contribution of bright sources to the total CXB discussed in Section 3.

Acknowledgements. BeppoSAX is a joint Italian-Dutch programme. MG acknowledges snd ESA Fellowship. We acknowledge support from the BeppoSAX SDC. We thank the referee, G.Hasinger for useful comments. SM thanks A.S.Comastri for useful discussions.

References

- Boella G., Butler R.C., Perola G.C., et al., 1997, A&AS 122, 299
- Boella G., Chiappetti, L., Conti, G., et al., 1997, A&AS 122, 327
- Chen L.-W., Fabian A.C., Gendreau K.C., 1997, MNRAS 285, 449
- Comastri A., Fiore F., Giommi P., et al., 1999, Ad.S.R., in press (astro-ph/9902060)
- Conti G., Mattaini E., Santambrogio E.B., et al., 1994, SPIE 2279, 101
- Dickey J.M., Lockman F.J., 1990, ARA&A 28, 215
- Fiore F., La Franca F., Giommi P., et al., 1999, MNRAS, 306, L55
- Fixsen D.J., Cheng E.S., Gales J.M., et al., 1996, ApJ, 473, 576
- Gendreau K., Mushotzky R., Fabian A.C., et al., 1995, PASJ 47, L5
- Georgantopoulos I., Stewart G., Shanks T., et al., 1996, MNRAS 280, 276
- Giacconi R., Gursky H., Paolini F. & Rossi, B., 1962, Phys. Rev. Lett. 9, 439
- Griffiths N.W., Jordan C., 1998, ApJ 497, 883
- Gruber D.E., Matteson J.L., Peterson L.E., Jung G.V. 1999, Report-no: SP-98-25 (astro-ph/9903492)
- Hasinger G., 1992, in: The X-ray Background, Barcons X., Fabian A.C., (eds.) Cambridge University Press, Cambridge, p. 299
- Hasinger G., Burg R., Giacconi R., et al., 1998, A&A 329, 482
- Marshall F.E., Boldt E.A., Holt S.S., et al., 1980, ApJ 235, 4
- McCammon D., Sanders W.T., 1990, ARAA 28, 657
- Mewe R., Gronenschild E.H.B.M., van den Oord G.H.J., 1985, A&AS 62, 197
- Miyaji T., Ishisaki Y., Ogasaka Y., et al., 1998, A&A 334, L13
- Parmar A.N., Martin D.D.E., Bavdaz M., et al., 1997, A&AS 122, 309
- Parmar A.N., Guainazzi M., Oosterbroek T., et al., 1999, A&A 345, 611 (P99)
- Sacco B., in BeppoSAX June 1999 EIWG meeting report

Schwartz D. & Gursky H. 1974 in: X-ray Astronomy, Giacconi R., Gursky H. (eds.) D. Reidel Publishing Company, Dordrecht, p. 359